

## CHAPTER IV

### RESULTS AND DISCUSSION

This chapter is divided into two main parts: the catalyst characterization and pyrolysis using commercial and synthesized catalysts. The particular results and discussion are presented in this chapter.

#### 4.1 Catalyst Characterization

##### 4.1.1 Characterization for Precursor

The synthesized zirconium glycolate was characterized by FTIR technique (Figure 4.1), showing the bands located at 2939 and 2873  $\text{cm}^{-1}$  assigned to the (C–H) stretching frequencies. The C–H deformation vibrations were attributed to the bands in the region of 1400–1200  $\text{cm}^{-1}$  of methylene groups. Sodium tris(glycozirconate) complex displays the band at 1090  $\text{cm}^{-1}$ , corresponding to the Zr–O–C stretching vibration mode, and 613  $\text{cm}^{-1}$  referring to the Zr–O stretching frequency.

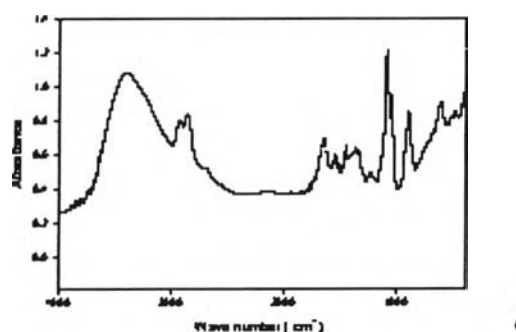


**Figure 4.1** FTIR spectrum of sodium tris(glycozirconate) complex.

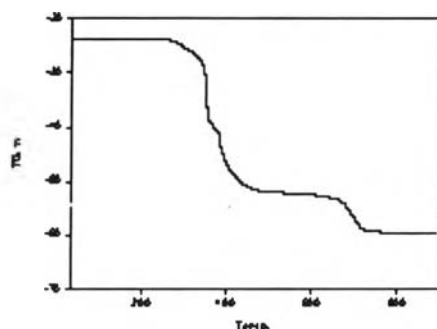


**Figure 4.2** TG thermogram of sodium tris (glycozirconate) complex.

The TG profile of sodium tris(glycozirconate) complex (Figure. 4.2) shows one major thermal decomposition ranging from 350°C to 545°C. Its weight loss of 41.59% corresponds to the conversion of as-synthesized product into carbon-free inorganic materials or to the decomposition of all organic ligands from the product framework. This experimental weight loss is consistent with the theoretical weight loss calculated for the formation of the proposed product,  $\text{Na}_2\text{O} \cdot \text{ZrO}_2$ , which is 41.67%. Therefore, the final percent ceramic yield of the product is 58.41%, which is in excellent agreement with the theoretical value of 58.33%.

#### 4.1.2 Characterization of Zirconia

Zirconia product synthesized via the sol-gel process was identified using XRD, as compared to a commercial one (Figure 4.3). The obtained zirconia illustrates the characteristic peak ( $2\theta = 30.2^\circ$ ) of tetragonal zirconia while the commercial one shows the monoclinic crystal structure.

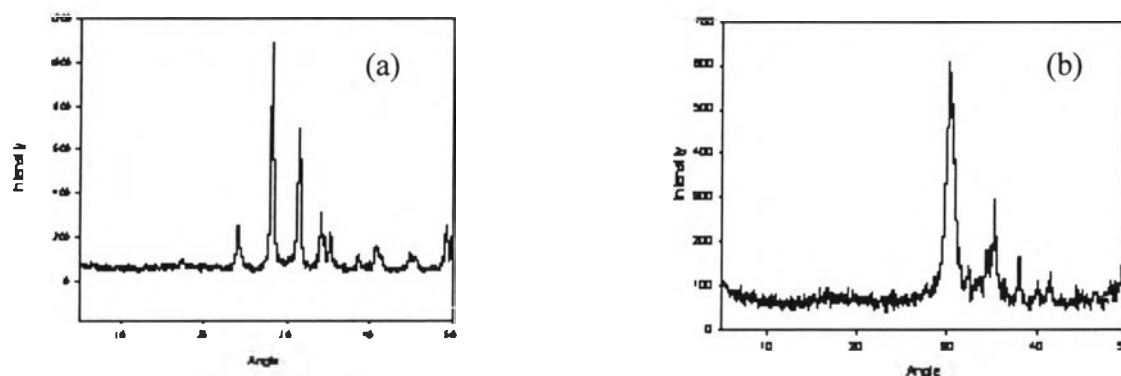


**Figure 4.3** XRD patterns of (a) commercial and (b) synthesized zirconias.

### 4.1.3 Characterization of $\text{SO}_4^{2-}/\text{ZrO}_2$

#### 4.1.3.1 *Thermal Stability of $\text{SO}_4^{2-}/\text{ZrO}_2$*

Figure 4.4 shows the weight loss of sulfated zirconia both commercial and synthesized catalysts, containing various percentages of sulfate loading (up to 8 wt. % sulfate). They have two regions of weight loss: the first one (30-500 °C) belong to the desorption of water on the surface of the catalyst and the second one (550-800 °C) shows the desorption of the sulfate ions (Davis *et al.*, 1994). Area under the curves in these regions relates to the amount of water and the concentration of sulfate ions impregnated on the surface of  $\text{ZrO}_2$  respectively. The higher surface area of  $\text{SO}_4^{2-}/$  synthesized  $\text{ZrO}_2$  leads to the higher amount of water to deposit and decompose from the surface of the catalyst. The results also indicate that all  $\text{SO}_4^{2-}/\text{ZrO}_2$  are still stable through the course of pyrolysis experiments performed up to 500 °C.

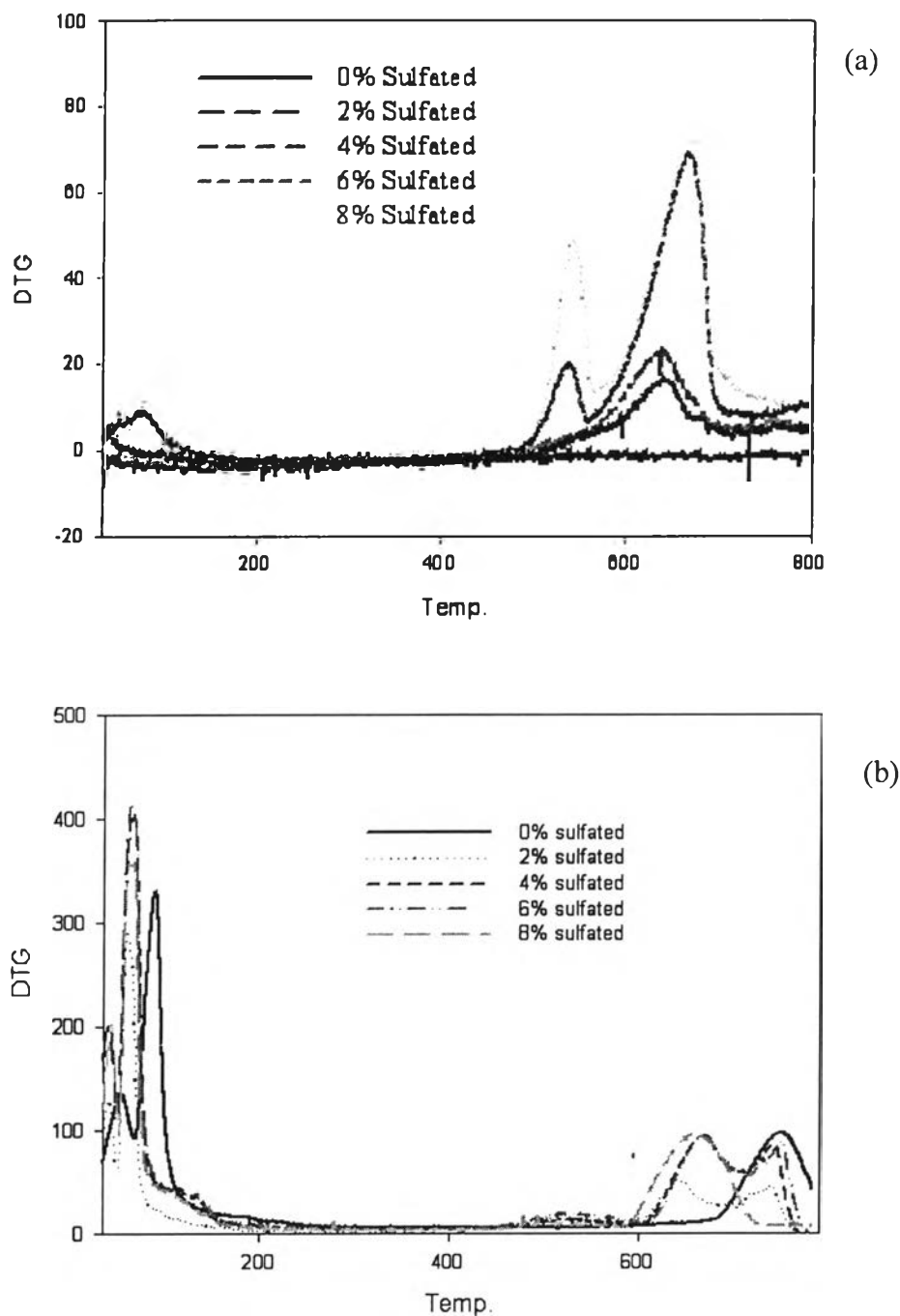


**Figure 4.4** DTG curves of (a)  $\text{SO}_4^{2-}$ /commercial  $\text{ZrO}_2$  and (b)  $\text{SO}_4^{2-}$ /synthesized  $\text{ZrO}_2$ .

#### 4.1.3.2 XRD Spectrum of Sulfated Zirconia

The XRD spectra of the commercial sulfated zirconia (Figure 4.5) indicate monoclinic crystal structure as the same as that of unloaded zirconia. The increasing percentage of sulfate has no effect on the crystal structure of the catalyst because the monoclinic is the most stable structure of zirconia. (Stichert *et al.*, 2001).

For the synthesized zirconia (Figure 4.6), the tetragonal crystal structure is observed, and after adding sulfate from 2% to 8% the intensity of XRD spectrum decreases and becomes broader. However, the tetragonal structure is still observed.

#### 4.1.4 Characterization of $\text{KNO}_3/\text{ZrO}_2$

##### 4.1.4.1 Thermal Stability of $\text{KNO}_3/\text{ZrO}_2$

Figure 4.7 shows the weight loss of potassium nitrate loaded zirconia containing various percentages of potassium loading (up to 30 wt. % potassium nitrate). The figure illustrates three regions of weight loss. The first one (30-300 °C) belongs to the desorption of water on the surface of the catalysts. The second region (300-600 °C) corresponds to the desorption of the potassium nitrate that does not form the interaction with the substrate. This region indicates to the host-guest interaction that makes  $\text{KNO}_3$  decompose around 600-800 °C (Wang *et al.*, 2000). The third region (>800 °C) belongs to the decomposition of  $\text{KNO}_3$ , which does not interact with the zirconia and still keeps the original property and needs high temperature over 800 °C for decomposition (Wang *et al.*, 2000).

And from the results,  $\text{KNO}_3$ /synthesized  $\text{ZrO}_2$  does not show the third region of decomposition due to the surface area higher than the commercial catalyst, so it has no non-interact  $\text{KNO}_3$  on the synthesized catalyst

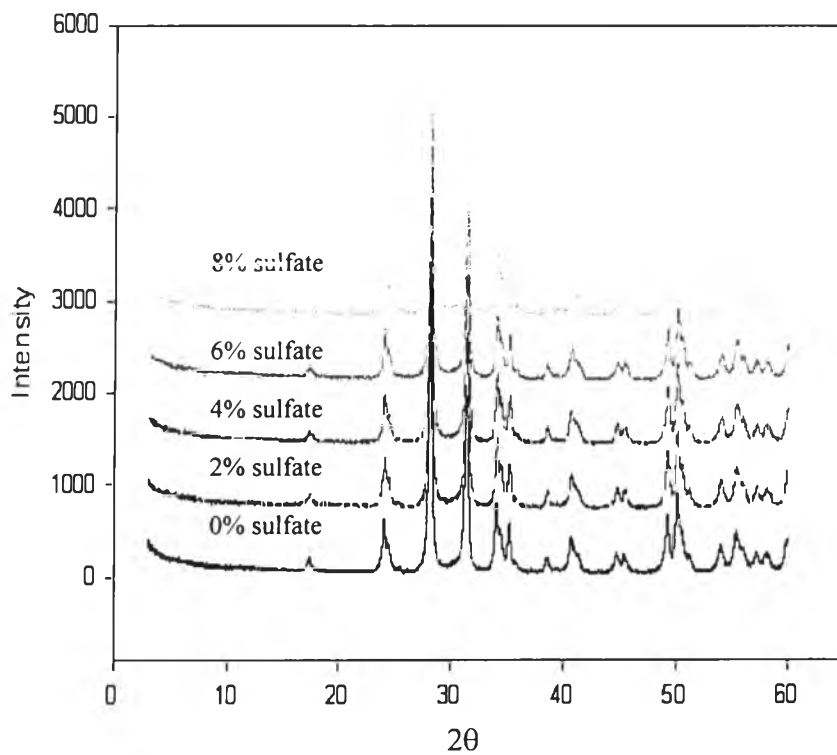


Figure 4.5 XRD spectra of  $\text{SO}_4^{2-}$ / commercial  $\text{ZrO}_2$ .

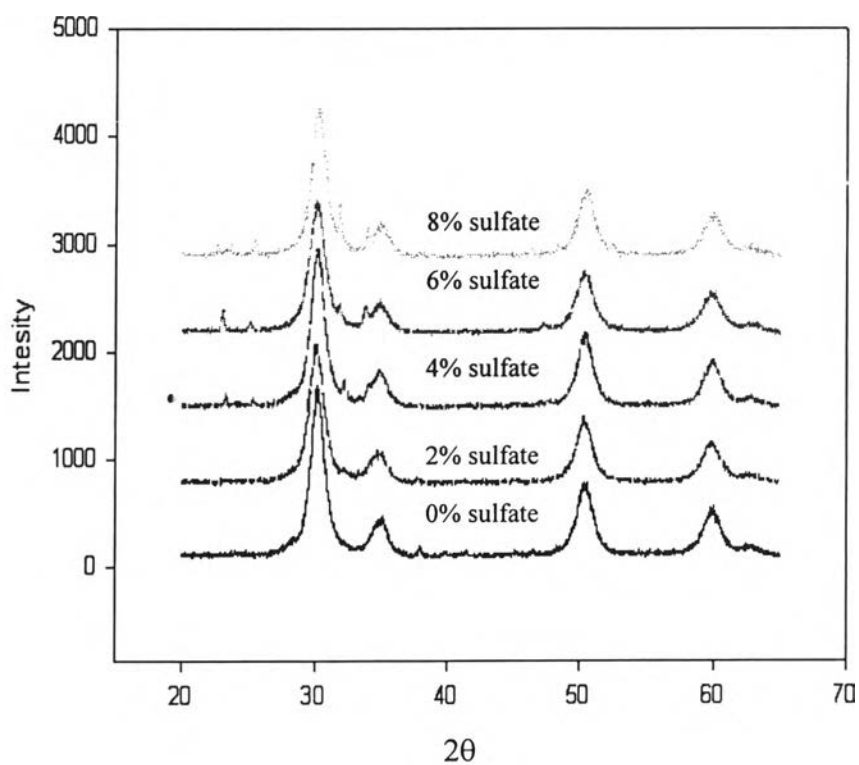


Figure 4.6 XRD spectra of  $\text{SO}_4^{2-}$ / synthesized  $\text{ZrO}_2$ .

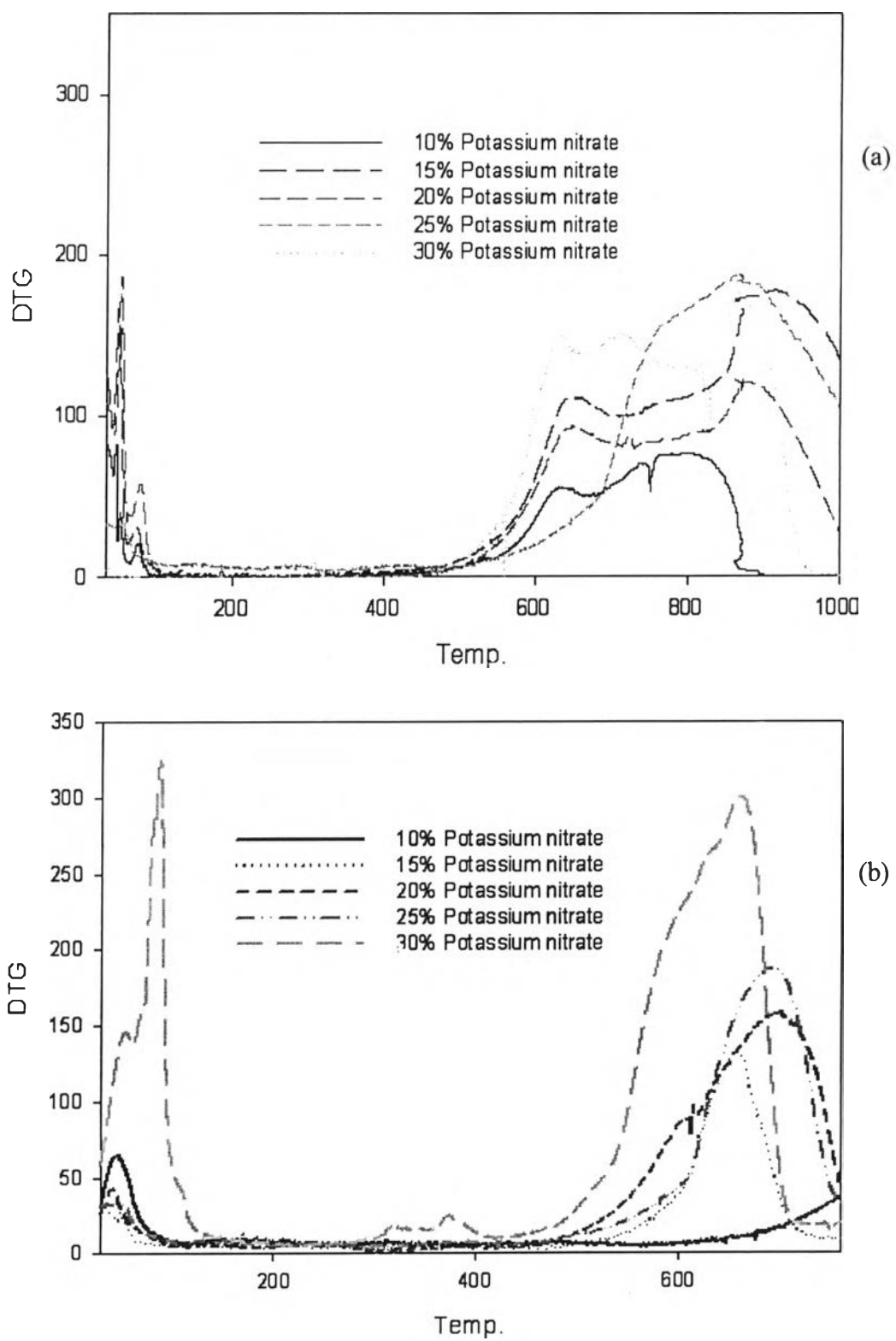


Figure 4.7 DTG curves of (a)  $\text{KNO}_3$ / commercial and (b)  $\text{KNO}_3$ / synthesized  $\text{ZrO}_2$ .

#### 4.1.4.2 XRD Spectrum of $KNO_3/ZrO_2$

The XRD spectra of the potassium nitrate loaded commercial zirconia (Figure 4.8) indicate monoclinic crystal structure, which is the same as that of unloaded one. The increasing percentage of potassium nitrate has no effect on the crystal structure of the catalyst because the monoclinic phase is the most stable phase of zirconia (Stichert *et al.*, 2001).

For the synthesized zirconia (Figure 4.9), the tetragonal crystal structure is observed. The characteristic peaks of  $KNO_3$  are observed ( $2\theta = 23.6^\circ$ ,  $29.4^\circ$  and  $33.8^\circ$ ) (Wang *et al.*, 2000). When the amount of loaded  $KNO_3$  increases, their intensities are raised. However, the tetragonal phase is still observed.



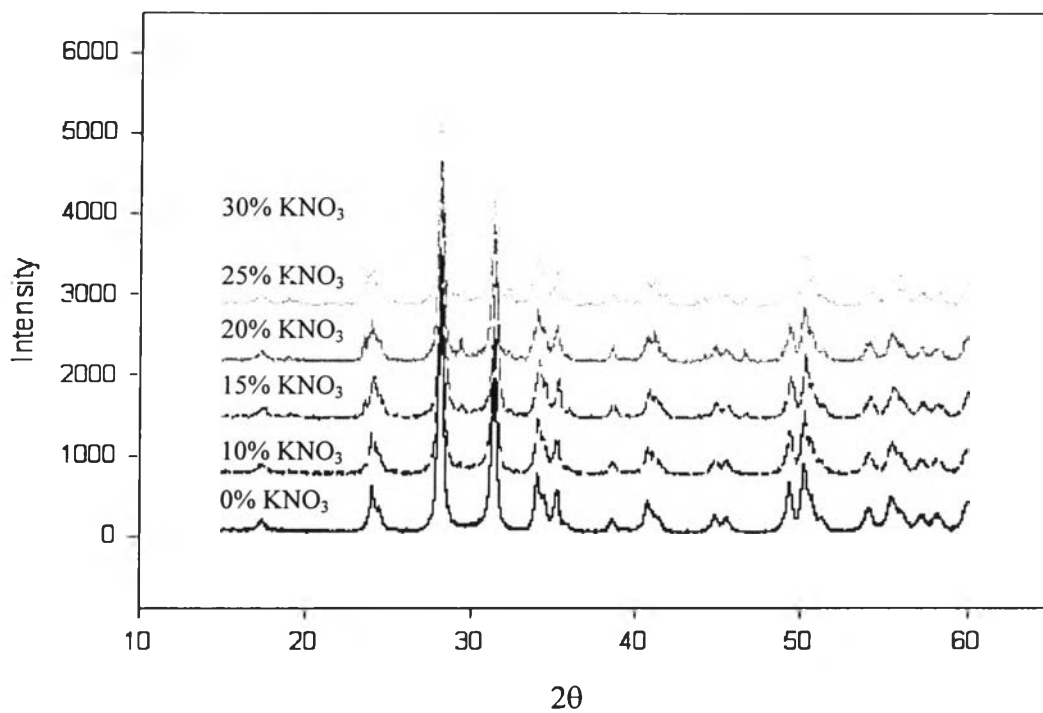


**Figure 4.8** XRD spectra of commercial  $\text{KNO}_3/\text{ZrO}_2$ .

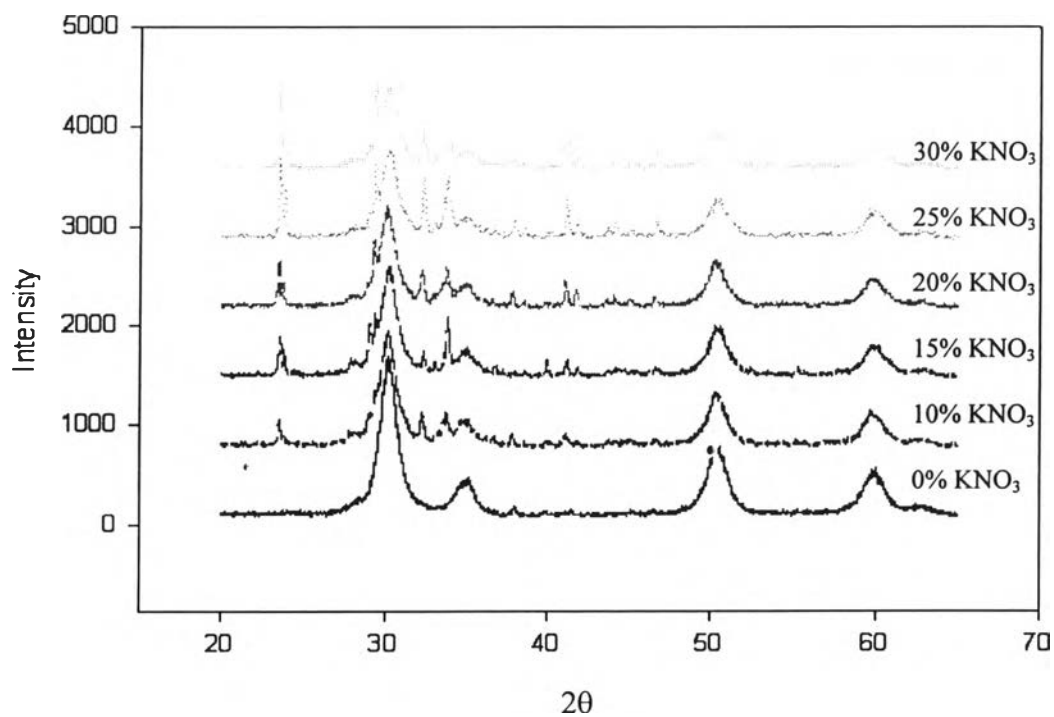


**Figure 4.9** XRD spectra of synthesized  $\text{KNO}_3/\text{ZrO}_2$ .

## 4.2 Effect of Commercial Catalysts on Pyrolyzed Products

### 4.2.1 Superacid Catalyst

Sulfated commercial zirconia ( $\text{SO}_4^{2-}$ /commercial  $\text{ZrO}_2$ ) was employed as a catalyst in this study. Pyrolyzed product distribution and composition were investigated with an increase of catalyst to polymer ratio and amount of sulfated loading, respectively.

#### 4.2.1.1. Product Yield

The catalyst to polymer ratio applied to the experiments in this section was 1:6 and 2:6. A total 0.5 gram of polyethylene (PE) film sample and catalyst were mixed together and loaded at the bottom of the reactor. The percentage of sulfate on the commercial  $\text{ZrO}_2$  was varied from 0 -8 %. Product yields after pyrolysis are shown in Figure 4.10. No residue production was observed. The liquid fraction was the most dominant degradation products both 1 to 6 and 2 to 6 catalyst to polymer ratio. Moreover, it was found that the gas yield increased and the liquid yield decreased as the percentage of sulfate increased in both cases.

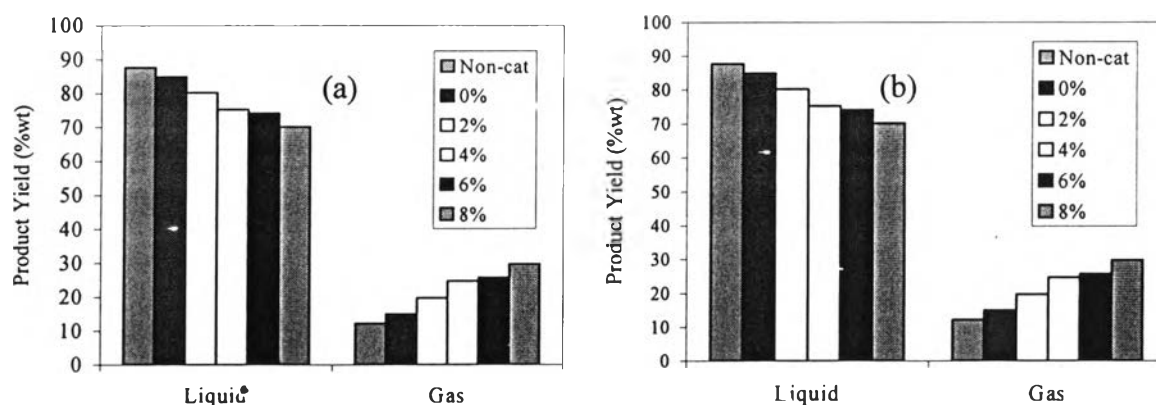


**Figure 4.10** Product yield from catalytic pyrolysis of PE film using  $\text{SO}_4^{2-}$ /commercial  $\text{ZrO}_2$  and the catalyst to polymer ratio of (a) 1:6 and (b) 2:6 at various percentages of sulfate.

#### 4.2.1.2 Gas Product Composition

Gaseous products were identified as methane, ethylene, ethane, propylene, propane, C<sub>4</sub>, C<sub>5</sub>, C<sub>6</sub>, C<sub>7</sub> and C<sub>8</sub> hydrocarbons as shown in Figure 4.11. In the catalyst to polymer ratio equal to 1 to 6, it shows the increase of every fractions along with increasing the percentage of sulfate whereas in the case of using catalyst to polymer ratio equals to 2 to 6, lighter hydrocarbons (methane to propylene) increase, but the heavier hydrocarbons (propane to C<sub>8</sub>) decrease along with the increasing percentage of sulfate.

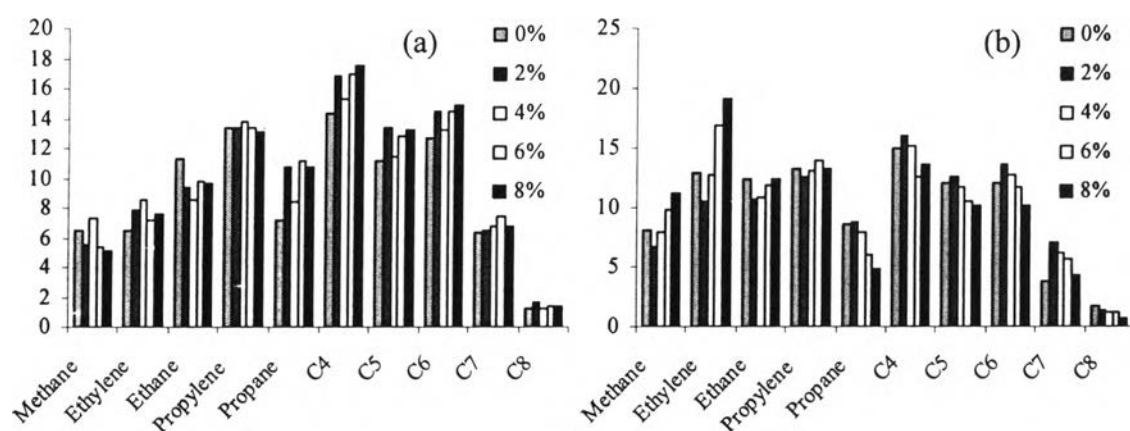


**Figure 4.11** Gas composition from catalytic pyrolysis of PE film using  $\text{SO}_4^{2-}/$  commercial  $\text{ZrO}_2$  and the catalyst to polymer ratio (a) 1:6 and (b) 2:6 at various percentages of sulfate.

#### 4.2.1.3 Liquid Product Composition

Compositions of the liquid products from pyrolysis of PE film with 1:6 and 2:6 catalyst to polymer ratio at various percentages of sulfates are shown in Figure 4.12. For thermal degradation and catalytic pyrolysis, the liquid products are distributed over a wide range of carbon numbers (C<sub>9</sub> to C<sub>49</sub>) equivalent to boiling point range of 68 to 560 °C. In the case of using sulfated zirconia with the various percentage of sulfates, the increase of the percentage resulted in an increase of lighter hydrocarbons in the both cases. However, the ratio of 2:6 shows more cracking activity of catalyst than the ratio 1:6, and the carbon number distribution of ratio equal to 2:6 is narrower than the ratio 1:6 by observing from the shape of peak.

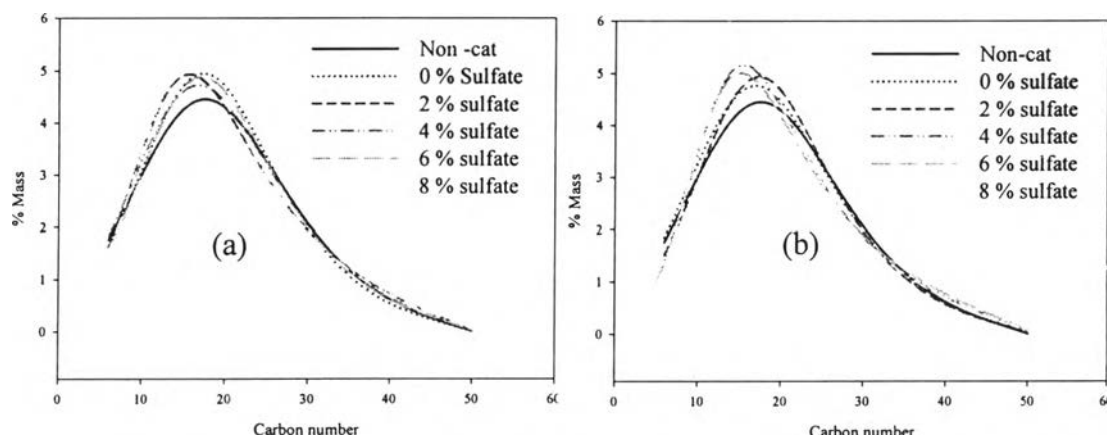


**Figure 4.12** Carbon number distributions of liquid products from thermal and catalytic degradation of PE film using  $\text{SO}_4^{2-}$ / commercial  $\text{ZrO}_2$  and the catalyst to polymer (a) 1:6 and (b) 2:6 at various percentages of sulfate.

#### 4.2.1.4 Oil Fractions of Liquid Product

Figure 4.13 shows the distribution of the liquid products from pyrolysis of PE film with 1:6 and 2:6 catalyst to polymer ratio at various percentages of sulfates. The fractions are defined according to the boiling points as gasoline (69-149 °C), kerosene (149-232 °C), gas oil (232-343 °C), light vacuum gas oil (343-371 °C) and heavy vacuum gas oil (371-559 °C). Thermal degradation gives the highest amount of the heaviest fraction, heavy vacuum gas oil, when compared with the catalytic ones. The major component in oil fractions for both catalyst to polymer ratio is gas oil, which slightly decreases along with increasing of the percentage of sulfate because the lighter fractions i.e. kerosene and gasoline increase.

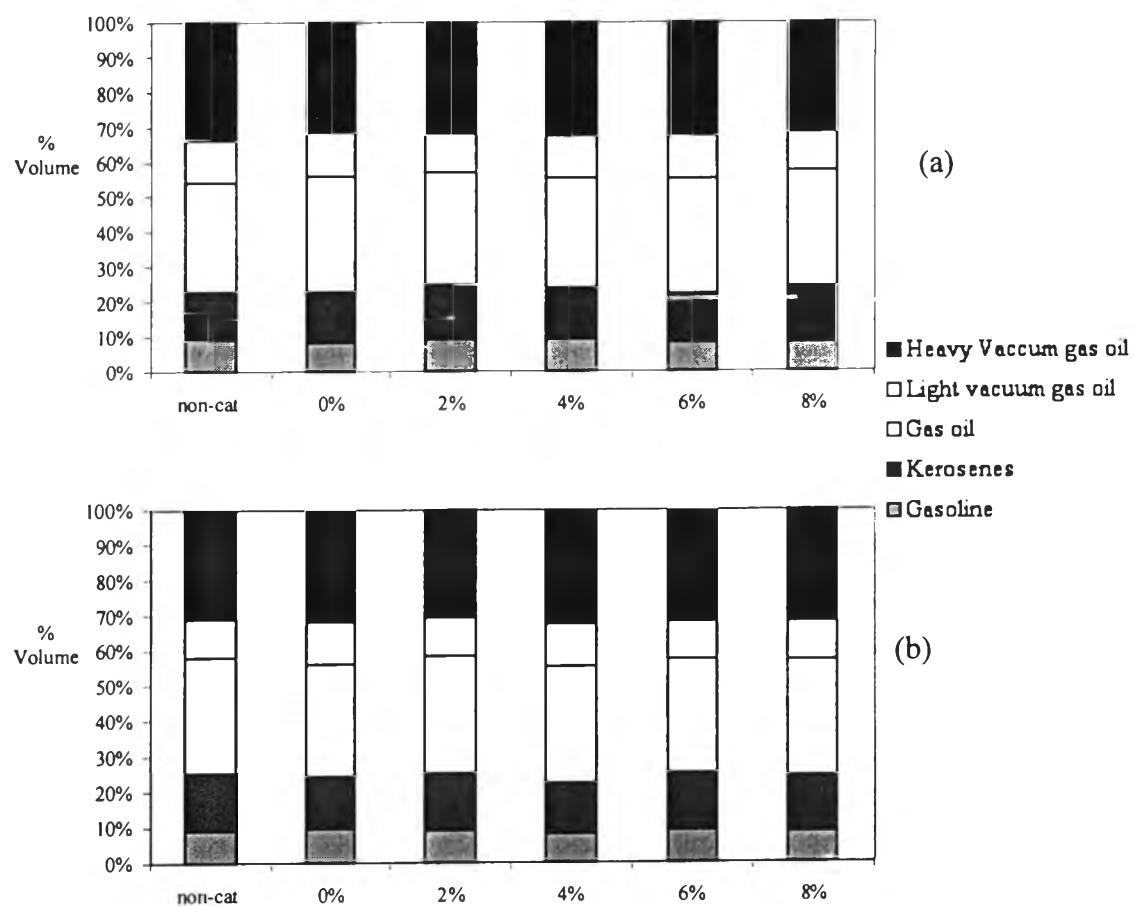


**Figure 4.13** Liquid fractions from thermal and catalytic degradation of PE film using  $\text{SO}_4^{2-}$ / commercial  $\text{ZrO}_2$  and the catalyst to polymer ratio of (a) 1:6 and (b) 2:6 at various percentages of sulfate.

#### 4.2.2 Superbasic Catalysts

Potassium nitrate loaded zirconia ( $\text{KNO}_3/\text{commercial ZrO}_2$ ) was employed as a catalyst in this study. Pyrolyzed product distribution and composition were investigated with an increase of catalyst to polymer ratio and amount of potassium nitrate loading, respectively.

##### 4.2.2.1. Product Yield

The catalyst to polymer ratio applied to the experiments in this section was 1:6 and 2:6. A total 0.5 gram of polyethylene (PE) film sample and catalyst were mixed together and loaded at the bottom of the reactor. The percentage of potassium nitrate was varied from 0 - 30 %. Product yields after pyrolysis are shown in Figure 4.14. In the presence of the  $\text{KNO}_3/\text{commercial ZrO}_2$  catalyst, the liquid yield decreases and intends to decrease more with the increasing percentage of potassium nitrate. Much greater effect of the catalyst can be observed at the higher catalyst to polymer ratio. From both cases, no residue was observed.

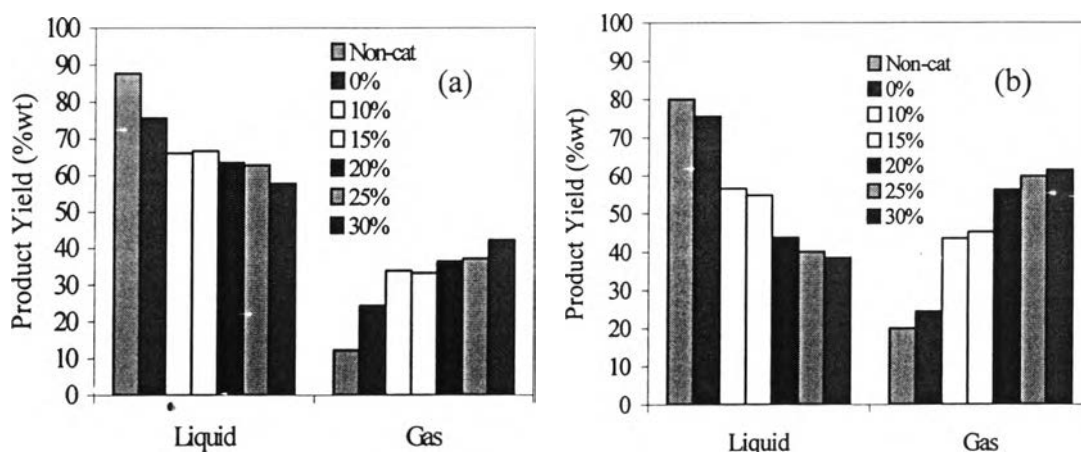


**Figure 4.14** Product yield from catalytic pyrolysis of PE film using  $\text{KNO}_3/\text{commercial ZrO}_2$  and the catalyst to polymer ratio of (a) 1:6 and (b) 2:6 at various percentages of potassium nitrate.

ต้นฉบับ หน้าขาดหาย

ต้นฉบับ หน้าขาดหาย



make the polymerization dominant in the reaction, so the result of oil fraction in this ratio followed the similar trend as the result from using superacid and non catalytic cases.

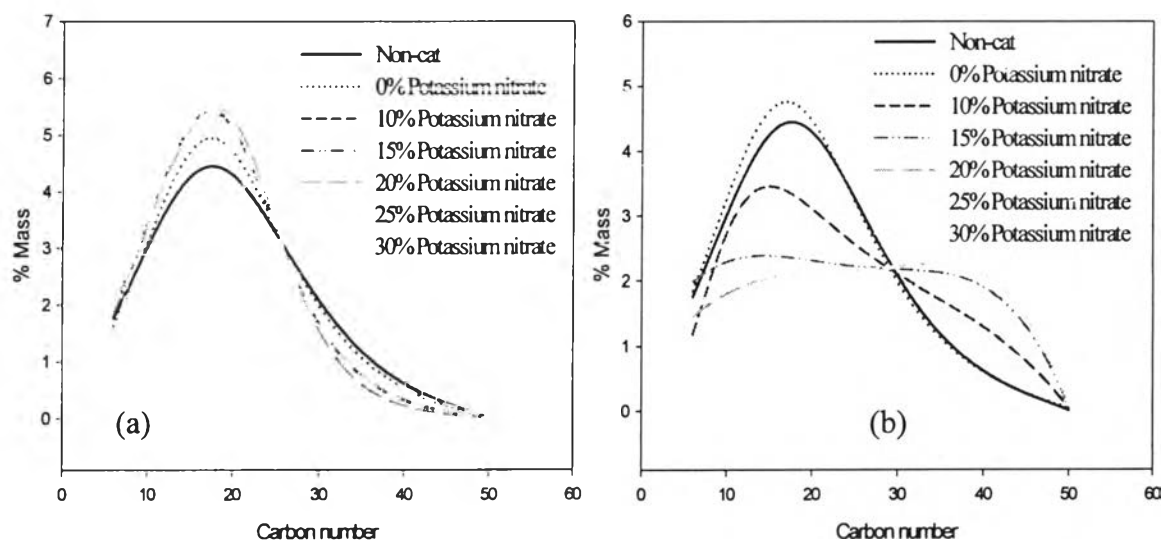


**Figure 4.16** Carbon number distributions of liquid products from thermal and catalytic degradation of PE film using  $\text{KNO}_3$ / commercial  $\text{ZrO}_2$  and the catalyst to polymer ratios of (a) 1:6 and (b) 2:6 at various percentages of potassium nitrate.

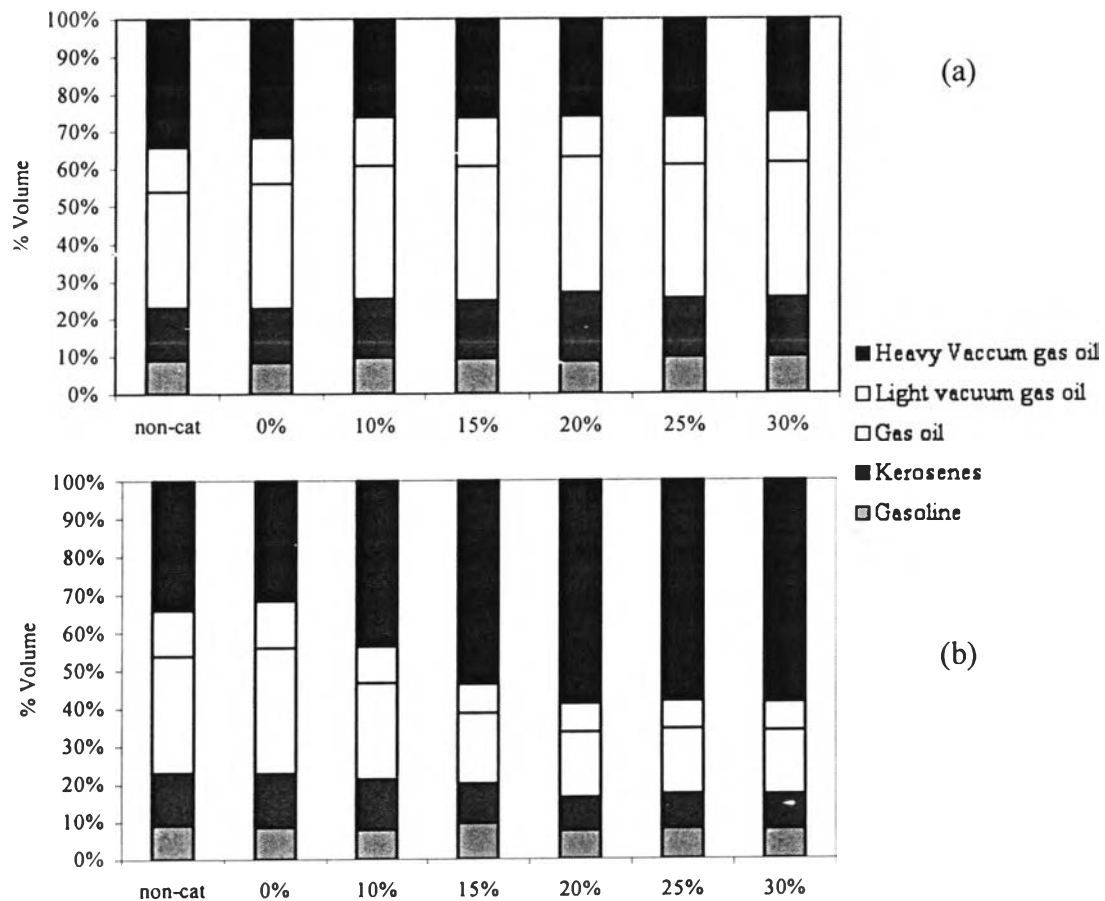


**Figure 4.17** Liquid fractions from thermal and catalytic degradation of PE film using  $\text{KNO}_3$ / commercial  $\text{ZrO}_2$  and the catalyst to polymer ratio of (a) 1:6 and (b) 2:6 at various percentages of potassium nitrate.

### 4.3 Effect of Synthesized Catalysts on Pyrolyzed Products

#### 4.3.1 Superacid Catalyst

Sulfated synthesized zirconia ( $\text{SO}_4^{2-}/$  synthesized  $\text{ZrO}_2$ ) was employed as a catalyst in this study. Pyrolyzed product distribution and composition were investigated with an increase of catalyst to polymer ratio and amount of sulfated loading, respectively.

##### 4.3.1.1 Product Yield

The catalyst to polymer ratio in this section was also 1:6 and 2:6. A total 0.5 gram of polyethylene (PE) film sample and catalyst were mixed together and loaded at the bottom of the reactor. The percentage of sulfate was varied from 0-8 %. Product yields after pyrolysis are shown in Figure 4.12. No residue production was observed. The gas fraction becomes the major degradation product using 1 to 6 catalysts to polymer ratio, and the higher amount is observed in the case of higher catalyst to polymer ratio of 2:6 due to the higher cracking activity of the tetragonal crystal structure in the synthesized catalyst.

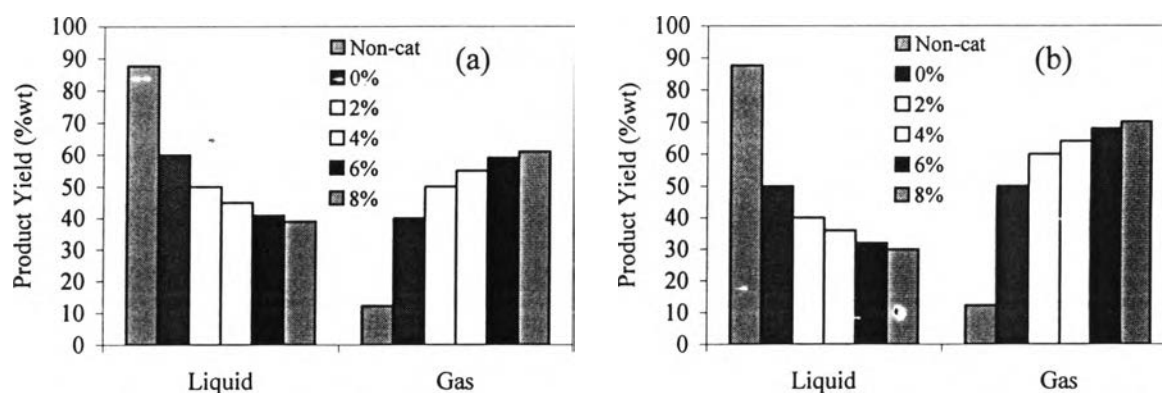


**Figure 4.18** Product yield from catalytic pyrolysis of PE film using  $\text{SO}_4^{2-}/$  synthesized  $\text{ZrO}_2$  and the catalyst to polymer ratio of (a) 1:6 and (b) 2:6 at various percentages of sulfate.

#### 4.3.1.2 Gas Product Composition

Figure 4.19 shows the significant increase in light hydrocarbons and the decrease in heavy hydrocarbons in the gas fraction produced from pyrolysis with the synthesized catalysts. The commercial catalysts did not give such a strong effect. Furthermore, with the ratio of 2:6, the C<sub>8</sub> fraction was almost eliminated from this product with the decrease to 1 %, due to the powerful cracking activity of the synthesized catalysts.

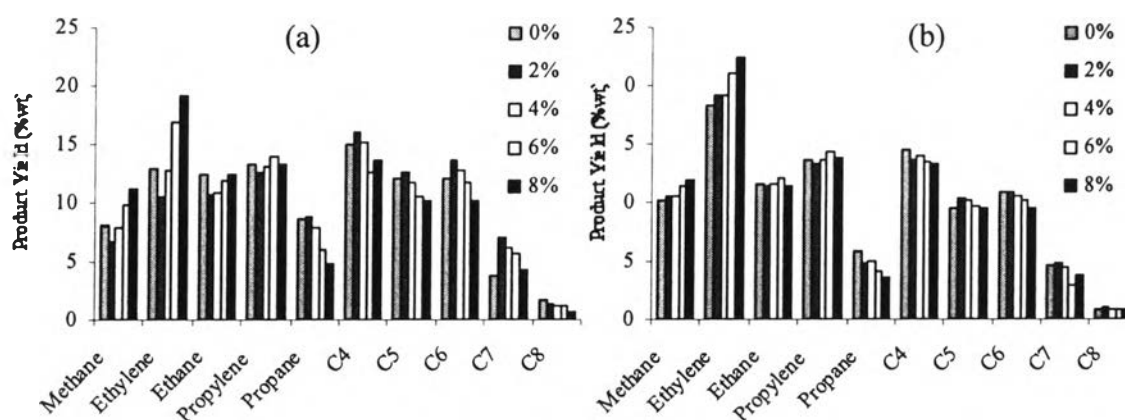


**Figure 4.19** Gas compositions from catalytic pyrolysis of PE film using synthesized  $\text{SO}_4^{2-}$ / synthesized  $\text{ZrO}_2$  and the catalyst to polymer ratio of (a) 1:6 and (b) 2:6 at various percentages of sulfate.

#### 4.3.1.3 Liquid Product Composition

Compositions of the liquid products from pyrolysis of PE film by using synthesized catalyst with 1:6 and 2:6 catalyst to polymer ratios at various percentages of sulfates are shown in Figure 4.20. In the case of using sulfated zirconia at the catalyst to polymer ratio 1:6, the distribution of carbon number shifts to the lighter hydrocarbon but not as much as the catalyst to polymer ratio 2:6. At 8 % of sulfate, the lowest carbon number distribution in both cases is observed.

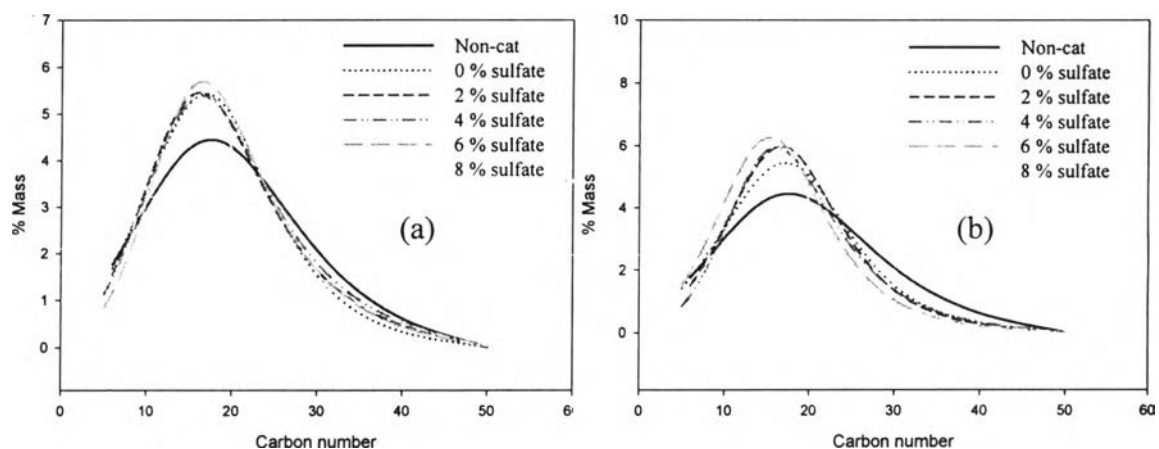


**Figure 4.20** Carbon number distributions of liquid products from thermal and catalytic degradation of PE film using  $\text{SO}_4^{2-}$ / synthesized  $\text{ZrO}_2$  and the catalyst to polymer ratios of (a) 1:6 and (b) 2:6 at various percentages of sulfate.

#### 4.3.1.4 Oil Fractions of Liquid Product

Figure 4.21 shows the distribution of the liquid products from pyrolysis of PE film with 1:6 and 2:6 catalysts to polymer ratio at various percentages of sulfates. At the highest percentage of sulfate, the lowest amount of the heavy vacuum gas oil, which is the heaviest fraction of the liquid product composition is observed, and the increase of the lighter fractions occurs along with the increasing of percentage of sulfate. The synthesized catalysts have the higher cracking activity than the commercial catalysts because the lower amount of vacuum gas oil fraction and the higher amount of the lighter fractions are observed. The increase of catalyst to polymer ratio and percentage of sulfate resulted in an increase of lighter hydrocarbons and increase in value of the pyrolyzed products.

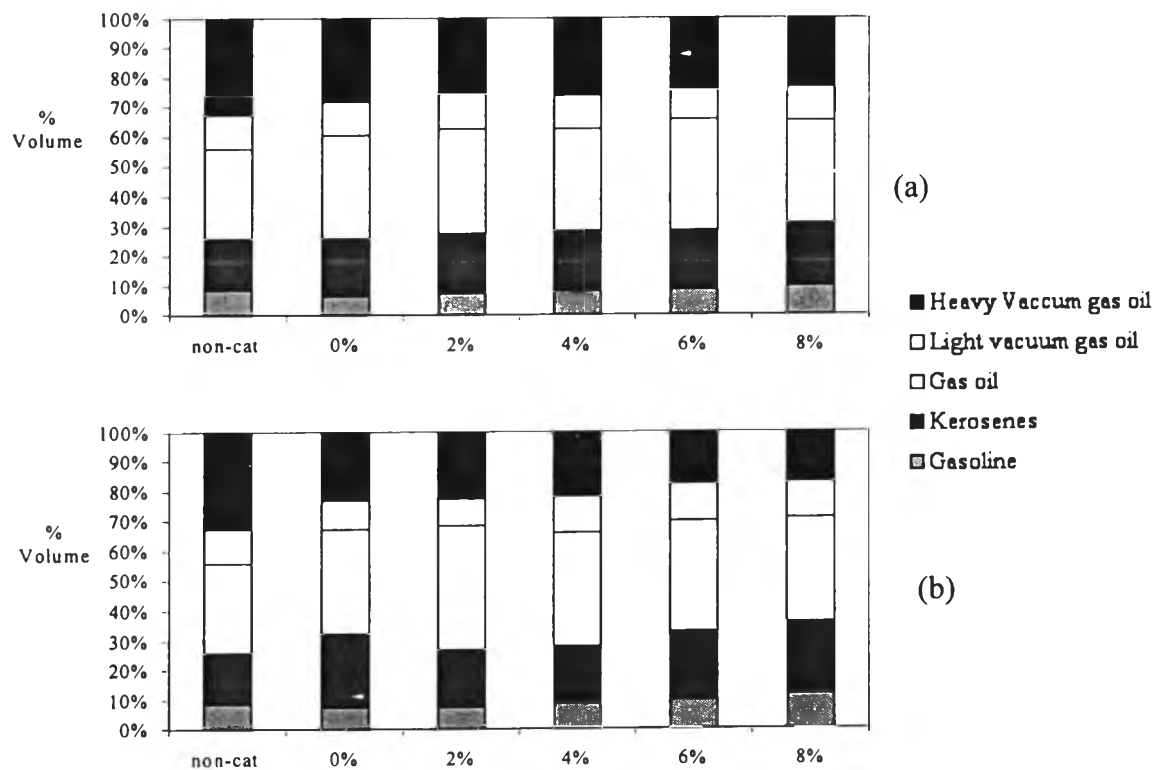


**Figure 4.21** Liquid fractions from thermal and catalytic degradation of PE film using  $\text{SO}_4^{2-}$ / synthesized  $\text{ZrO}_2$  and the catalyst to polymer ratio of (a) 1:6 and (b) 2:6 at various percentages of sulfate.

### 4.3.2 Superbasic Catalysts

Potassium nitrate loaded zirconia ( $\text{KNO}_3/\text{ZrO}_2$ ) was employed as a catalyst in this study. Pyrolyzed product distribution and composition were investigated with an increase of catalyst to polymer ratio and amount of potassium nitrate loading, respectively.

#### 4.3.2.1. Product Yield

In the presence of the  $\text{KNO}_3$ / synthesized  $\text{ZrO}_2$  catalyst, the liquid yield was increased at the beginning and intended to decrease with the higher percentage of potassium nitrate for both commercial and synthesized zirconia catalysts. Greater effect of the catalyst can be observed at the higher catalyst to polymer ratio. From both cases, no residue was observed, but the gas fraction was not the major fraction opposite to that observed from previous results. The amount of gas produced from using the catalyst to polymer ratio 2:6 was slightly higher than the gas produced using the catalyst to polymer ratio of 1:6. The observations are illustrated in Figure 4.22.

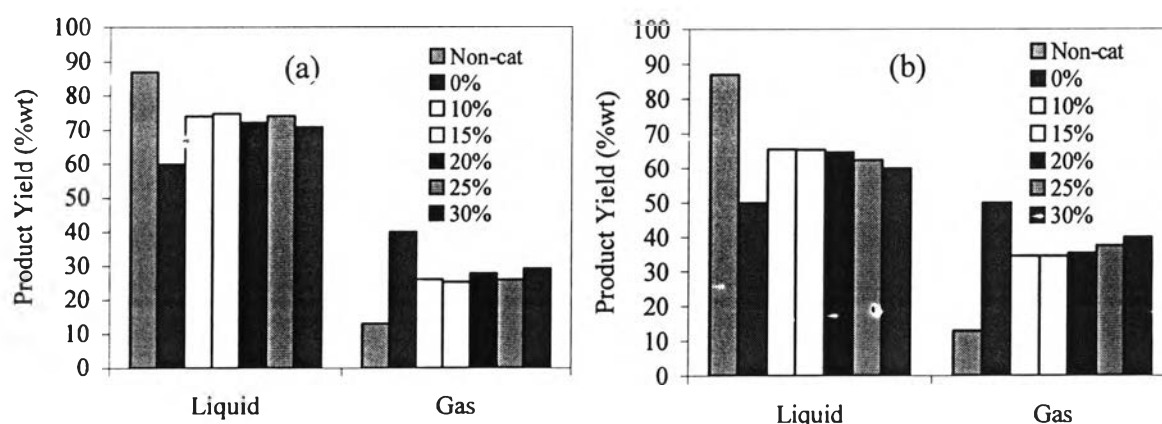


**Figure 4.22** Product yield from catalytic pyrolysis of PE film using  $\text{KNO}_3$ /synthesized  $\text{ZrO}_2$  and the catalyst to polymer ratio of (a) 1:6 and (b) 2:6 at various percentages of potassium nitrate.

#### 4.3.2.2 Gas Product Composition

Figure 4.23 shows the gas composition obtained from the catalytic of PE using  $\text{KNO}_3$ / synthesized  $\text{ZrO}_2$  at various percentages of potassium nitrate and the catalyst to polymer ratio of 1:6 and 2:6. After pyrolysis,  $\text{C}_4$  and  $\text{C}_6$  turn to be the major fractions of gas product, resulting in the dramatical decrease in methane and ethylene fractions using both catalyst to polymer ratios. The higher amount of heavier hydrocarbon fractions ( $\text{C}_4$ - $\text{C}_8$ ) is observed as compared to the thermal degradation case, using sulfated zirconia and commercial  $\text{KNO}_3/\text{ZrO}_2$  as catalysts.

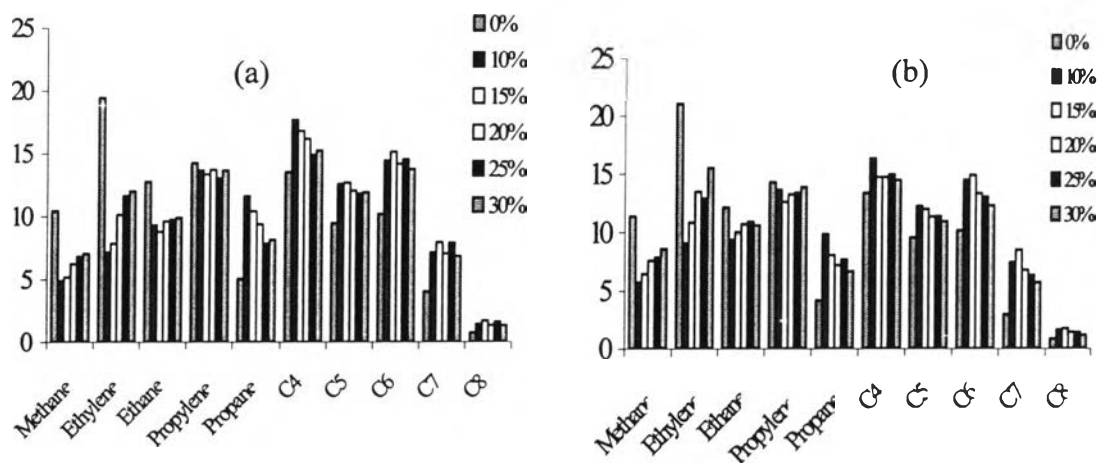


**Figure 4.23** Gas compositions from catalytic pyrolysis of PE film using  $\text{KNO}_3$ /synthesized  $\text{ZrO}_2$  and the catalyst to polymer ratio of (a) 1:6 and (b) 2:6 at various percentages of potassium nitrate.



### 4.3.2. Liquid Product Composition

Compositions of the liquid products from using  $\text{KNO}_3$ /synthesized  $\text{ZrO}_2$  are shown in Figure 4.24. For both catalysts to polymer ratio 1:6 and 2:6, the distribution of carbon number shifts to heavier hydrocarbons. The increasing percentages of potassium nitrate resulted in the decrease of lighter hydrocarbons. This result was possibly caused by the basicity of the catalyst that can generate the carboanion in the reaction, and the anionic polymerization could be occurred, resulting in products with higher molecular weight (Kijenski *et al.*, 2001). From the results, the higher catalyst to polymer ratio provides the higher catalytic activity of the catalyst.

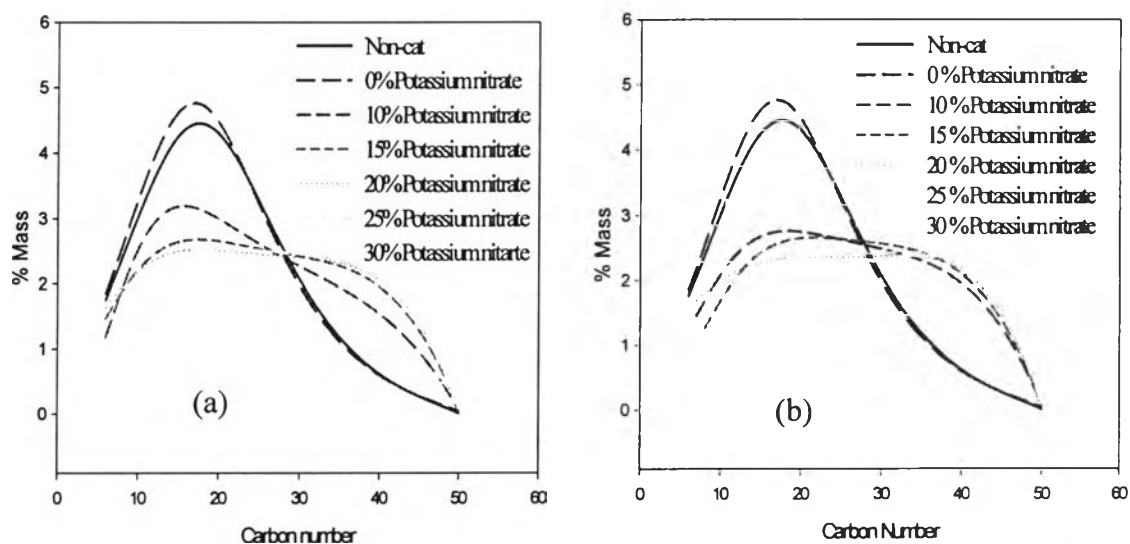


**Figure 4.24** Carbon number distributions of liquid products from thermal and catalytic degradation of PE film using  $\text{KNO}_3$ / synthesized  $\text{ZrO}_2$  and the catalyst to polymer ratios of (a) 1:6 and (b) 2:6 at various percentages of potassium nitrate.

#### *4.3.1.4 Oil Fractions of Liquid Product*

Figure 4.25 shows the distribution of the liquid products from pyrolysis of PE film with 1:6 and 2:6 catalysts to polymer ratio at various percentages of potassium nitrate. The heavy vacuum gas oil is the major component in both catalyst to polymer ratios. This result followed the same trend as in the previous section due to the polymerization of the cracked fractions occurred by the nature of superbase catalyst. The carboanion was generated in the reaction and the anionic polymerization took place to form higher molecular weight products instead of lower molecular weight ones. Due to the tetragonal phase of synthesized  $ZrO_2$ , the products at the catalyst to polymer ratio of 1:6 gave the different results when compared with the commercial catalyst at the same catalyst to polymer ratio.

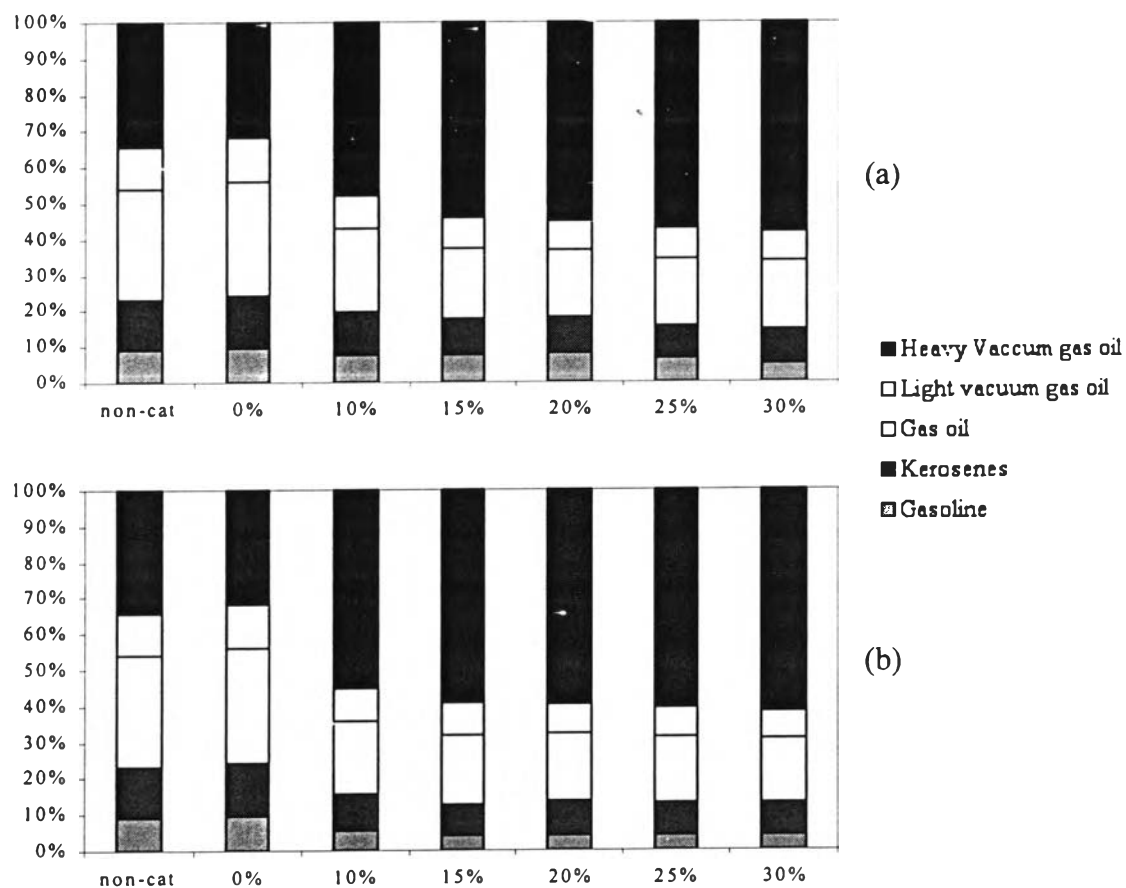


**Figure 4.25** Liquid fractions from thermal and catalytic degradation of PE film using  $\text{KNO}_3$ / synthesized  $\text{ZrO}_2$  and the catalyst to polymer ratios of (a) 1:6 and (b) 2:6 at various percentages of potassium nitrate.